

Soft X-Ray Measurement of the TPE-RX Reversed Field Pinch Plasma Using High Spectral Resolution TES Microcalorimeter

SHINOZAKI Keisuke, HOSHINO Akio, ISHISAKI Yoshitaka, MORITA Umeyo, OHASHI Takaya, MIHARA Tatehiro¹, MITSUDA Kazuhisa^{2,3}, TANAKA Keiichi³, YAGI Yasuyuki⁴, KOGUCHI Haruhisa⁴, HIRANO Yoichi⁴ and SAKAKITA Hajime⁴

Department of Physics, Tokyo Metropolitan University (TMU), Tokyo 192-0397, Japan

¹ *Cosmic Radiation, the Institute of Physical and Chemical Research, Wako 351-0198, Japan*

² *Institute of Space and Astronautical Science (ISAS/JAXA), Sagami-hara 229-8510, Japan*

³ *SII Nano-Technology Inc. (SIINT), Matsudo 270-2222, Japan*

⁴ *National Institute of Advanced Industrial Science and Technology (AIST), Tsukuba 305-8568, Japan*

(Received: 5 October 2004 / Accepted: 10 January 2006)

Abstract

We report the first result of soft X-ray spectroscopy for the Reversed Field Pinch (RFP) plasma in TPE-RX using a high spectral resolution (FWHM ~ 50 eV) superconductive transition edge sensor (TES) microcalorimeter. Total 3472 count of X-ray signals were detected in 0.2–3.0 keV for 210 plasma shots during the flat-top phase (35–70 ms) after the pile-up rejection. Combined with the 1.3–8 keV range data with a SiLi detector, we examined the wide band X-ray spectrum of the RFP plasma. The obtained spectrum is dominated by thermal plasma emission in the soft X-ray band ($\lesssim 5$ keV), although at least four different temperature component is required to account for the whole band spectral shape. The average temperature is consistent with the value by the ruby laser Thomson scattering method. The spectrum also indicates that 85% of the flux in 0.7–1.2 keV is dominated by the Fe-L complex with variously ionized states, and that the iron abundance to deuterium is comparable to the value derived for carbon and oxygen with a VUV spectrometer.

Keywords:

reversed field pinch, TPE-RX, X-ray, TES, microcalorimeter

1. Introduction

In the soft X-ray energy range of 0.2–8 keV, there exist K and L emission lines and absorption edges from various elements, *e.g.*, C, O, Cr, and Fe, which contain much information on the physical state of the X-ray emitting plasma (*e.g.*, temperature, density), element abundance, and motion of ions. A typical energy difference between the fine structures of these lines is 5–20 eV, hence a spectrometer with an energy resolution of a few eV is strongly desired to resolve them. For practical applications, it is also required to sustain a high count rate ($\gtrsim 1$ kc/s). Recently, a transition edge sensor (hereafter TES) was proposed as an extremely sensitive thermometer for X-ray microcalorimeters [1]. TES microcalorimeters also have a merit that the response time is significantly improved due to a strong electro-thermal feedback [2]. We are now developing a TES microcalorimeter array for future Japanese X-ray astronomy missions [4,8]. To date, an energy resolution of ~ 6 eV in the energy range of $\lesssim 10$ keV has been achieved with a single pixel device in our laboratory [3].

The TES microcalorimeter is a detector which measures energy of an incident X-ray photon as a temperature rise using the sharp transition edge of superconductors. To give its maximum performance, the detector must be cooled below ~ 100 mK by an adiabatic demagnetization refrigerator (ADR). We have also developed a portable ADR system for ground experiments, which is based on the system originally designed for the rocket experiment [6]. Temperature stability of $\lesssim 10$ μ K and holding time of ~ 24 h at 125 mK are attained so far.

This paper presents the first result of a new collaboration between the astrophysics and the fusion plasma fields. The deuterium plasma radiation and impurity line emissions from a large RFP device, the TPE-RX experiment [12,11], are investigated using the TES microcalorimeter installed in the ADR, which is directly connected to TPE-RX with a vacuum duct. TPE-RX is one of the three largest RFP machines in the world with major radius $R = 1.72$ m and minor radius $a = 0.45$ m.

The primary purpose of the experiment is resolving characteristic X-ray lines of impurities (*e.g.*, O, Cr, Fe, Mo) in 0.2–8 keV to evaluate the contribution of line intensities to the continuum spectrum.

2. Experimental setup

The TES is made of a thin bilayer film of titanium (40 nm thick) and gold (110 nm) with $0.5 \text{ mm} \times 0.5 \text{ mm}$ size, which is suspended by a silicon-nitride bridge ($1 \mu\text{m}$ thick $700 \mu\text{m}$ wide) as a weak thermal link to the silicon substrate. An X-ray absorber made of gold ($0.3 \text{ mm} \times 0.3 \text{ mm}$ wide, 300 nm thick) is deposited on the TES, and a sapphire collimator with $0.2 \text{ mm}\phi$ $300 \mu\text{m}$ thick is attached in front of the absorber. Detailed design, fabrication and its best performance are described in [3,10]. The TES microcalorimeter was installed in the ADR which was horizontally connected to No.15 port section of TPE-RX with a vacuum duct as shown in Fig. 1. The distance between the inner vessel and the detector surface was 2.40 m. We set seven orifices ($32 \text{ mm}\phi$, 3 mm thick), to avoid stray X-ray detection by the reflection inside the duct. An adjustable slit is placed at the port section to regulate the X-ray flux, which was fixed to 5 mm width 0.5 mm height during the measurement. There is a set of five aluminized mylar films (Al : 37 nm, $\text{C}_{10}\text{H}_8\text{O}_4$: 540 nm) in series inside the ADR for thermal and optical shielding to block infrared to ultraviolet light. The detector efficiency, including the entrance window transmission and the TES microcalorimeter quantum efficiency, is indicated in Fig. 3 (d). The TPE-RX vacuum vessel is made of stainless steel SUS316L (Fe: 66 %, Cr: 17 %, Ni: 14 %). Inside the vessel, many mushroom-type molyb-

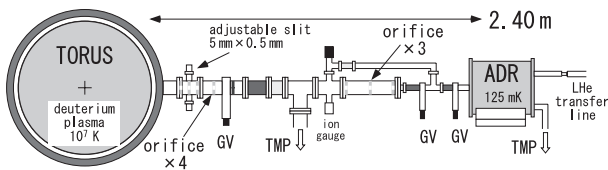


Fig. 1 The experimental setup between the ADR and TPE-RX.

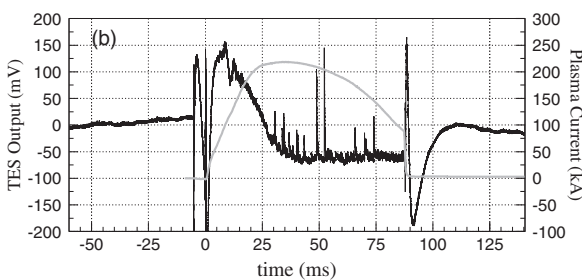


Fig. 2 A typical waveform during a plasma shot (black) and the plasma current (gray).

denum limiters ($98.5 \text{ mm}\phi$) are attached for the purpose of protection against the strong heat load. Total number of limiters is 244, and 34 are installed in the port section.

The measurement was conducted on 16–18 Aug 2004 at AIST and 210 plasma shots were obtained with a sufficient quality for the analysis. Each shot was basically generated in every 5 min interval, which is determined by the TPE-RX specifications. The deuterium gas pressure was kept constant at 0.4 mTorr during the discharge, and the plasma current I_p was $\sim 220 \text{ kA}$ during the flat-top phase (Fig. 2). Typical plasma parameters on this condition is that electron density $n_{el} = 5 \times 10^{18} \text{ m}^{-3}$, electron temperature $T_{el} = 600 \text{ eV}$, ion temperature $T_i = 300 \text{ eV}$, and the plasma beta $\beta_p = 0.07$ [11]. The ADR was cooled down to 125 mK and the TES was operated at $58 \text{ m}\Omega$ with the bias voltage of $2.4 \mu\text{V}$. In fact, the operating temperature and resistance are slightly higher than the optimal point, because we found a significant increase of low-frequency noise when the TES current was increased. In order to calibrate the detector gain continuously, a ^{55}Fe radioactive isotope was installed inside the ADR at an adequate position not obstructing the line of sight but the 5.9 keV (Mn- $K\alpha$) X-rays from the isotope coming into the detector. The count rate was about 0.09 c/s, which is enough to monitor the gain, while the probability that X-rays from the isotope came into the detector during the plasma shot ($< 100 \text{ ms}$) is negligible. From the analysis of the calibration isotope data, it is demonstrated that the energy resolution (FWHM) was $19.2 \pm 0.8 \text{ eV}$ at 5.9 keV and $14.6 \pm 0.3 \text{ eV}$ at 0 keV. However, it is found that the energy resolution was degraded to $\sim 50 \text{ eV}$ during the plasma shots due to the noise increase probably affected by the changes of the magnetic field generated by the plasma current.

3. Data analysis and results

Figure 2 shows the typical waveform of the TES microcalorimeter output obtained by a digital oscilloscope (2 MHz sample rate, 13 bit resolution) during a plasma shot. The waveform acquisition is triggered by the plasma current generation at $t = 0$ of the x-axis. The X-ray pulses from the detector have a shape of exponential decay $\propto \exp(-t/\tau_{eff})$, in which $\tau_{eff} \approx 200 \mu\text{s}$ throughout our measurement. When the gate valve was opened, soft X-ray signals were detected around 20–80 ms, while there were not when closed. We accumulate the X-ray pulses in the time duration of 35–70 ms corresponding the flat-top of I_p to make an energy spectrum. The energy of each pulse is determined by the optimal filtering method commonly used for the

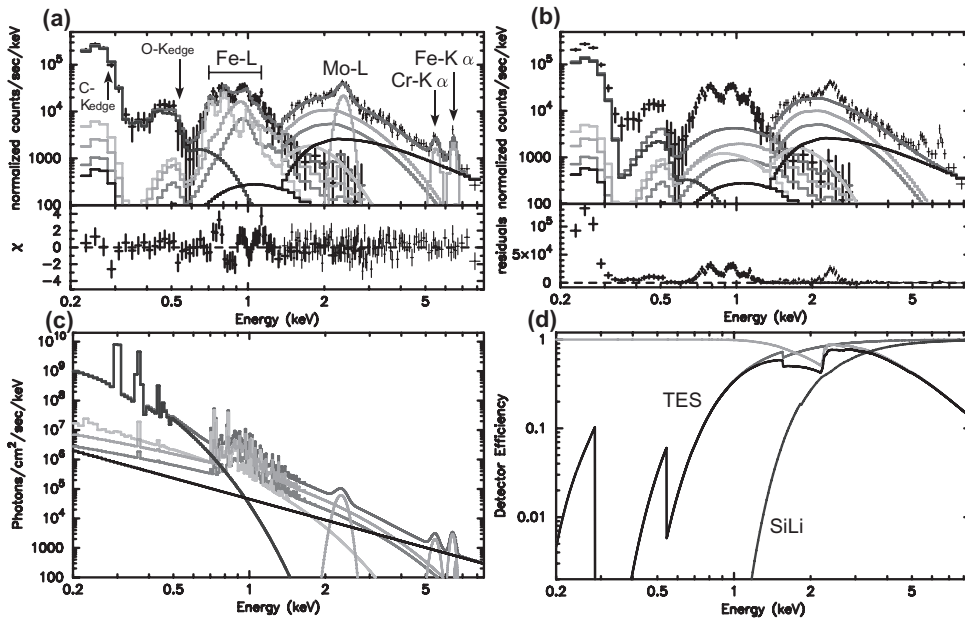


Fig. 3 (a) The TES (thick crosses) and SiLi (thin crosses) spectra fitted with the best fit model. (b) Same as (a), but without impurities lines. (c) The best fit model and each component. (d) Detector efficiencies of the TES microcalorimeter and SiLi including the window transmission and the detector quantum efficiency.

microcalorimeter pulse analysis [9]. The average and standard deviation of the detected count per shot are 23 ± 5 c/shot, corresponding to ~ 660 c/s. The pile-up events are rejected using the time interval between the two sequent events to be greater than $200 \mu\text{s}$. We also rejected pulses whose shape deviates significantly from the pulse template. As a result, 3472 count per 210 shots (7.35 s exposure) remains in the energy range of 0.2–3 keV, after rejecting 948 pulses. The obtained energy spectrum is indicated in Fig. 3 (a). In the spectral analysis, we also utilize a spectrum which was obtained with a SiLi detector at the same port with similar parameters of TPE-RX in October 2003. The SiLi detector has 4 mm ϕ aperture with 4.48 mm thick and the energy resolution is ~ 200 eV at 5.9 keV. A beryllium window with 87.7 μm thick was placed in front of the detector to constrain signals in hard band (see Fig. 3d). There are 4513 count per 16 shots (0.56 s) in 1.3–8 keV.

These spectra are examined using a spectral fitting package XSPEC v11.3 (<http://xspec.gsfc.nasa.gov/>), which is commonly used in the X-ray astronomy field. A thermal equilibrium plasma emission model, MEKAL [7], is used to account for the incident X-ray spectrum. Figure 3 (c) represents the best fit model, which is overlaid on Fig. 3 (a) after convolving the detector response. At least 4 thermal plasma + 1 power-law + 3 gaussian components are required to obtain a reasonable fit with $\chi^2/d = 203.0/151$ (d is a degree of freedom). Emissions from impurities in plasma are considered in the MEKAL model for C, O, Fe, and Ni, and the abundance ratio of Fe/Ni is fixed for the SUS316L

value. The TES microcalorimeter and the SiLi detector spectra are fitted simultaneously with the same model parameters except for the overall normalization. Number of fitting parameters are 23 in total. The best fit parameters are summarized in Table 1.

4. Discussion

The obtained X-ray spectra require at least four temperature component, ~ 78 , 350, 814, and 900 eV, plus power-law with photon index $\Gamma \sim 2.4$. The non-thermal power-law component is only visible at hard band (≥ 5 keV), and the soft X-ray band is dominated by the thermal plasma emission. There are little difference between the spectrum in the 35–50 ms duration and that in 50–70 ms, although the latter is slightly harder than the former. It is suggested that there would be temperature gradient from the plasma center to the edge in the line of sight. If we ignore the 78 eV component, the average temperature of the plasma is 550 eV, weighted with the MEKAL model normalization $\propto \int n_e n_i dV$. This temperature is consistent with the value (~ 600 eV) by the ruby laser Thomson scattering method.

Although three lines are detected in the SiLi spectrum, their line center energies are consistent with neutral Mo-L (2293 eV), Cr-K (5415 eV), and Fe-K (6404 eV), respectively. Their origins are thought to be fluorescence X-rays from the molybdenum limiters and the SUS316L vessel hit by high energy electrons. On the other hand, 85 % of the flux in 0.7–1.2 keV is dominated by Fe-L complex, and probably Cr-L, at variously ionized states (Fig. 3 (b)). This is a clear evidence that

Table 1 List of the best fit parameters

MEKAL model: $F_X = 8.79 \text{ erg cm}^{-2} \text{ s}^{-1}$ (0.2–10 keV)		
$kT_1 = 78_{-10}^{+10} \text{ eV}$,	$norm_1 = 75000_{-14000}^{+18000}$,	$F_X = 8.364$
$kT_2 = 350_{-48}^{+33} \text{ eV}$,	$norm_2 = 477_{-126}^{+105}$,	$F_X = 0.22$
$kT_3 = 814_{-78}^{+124} \text{ eV}$,	$norm_3 = 85_{-84}^{+35}$,	$F_X = 0.06$
$kT_4 = 900_{-820}^{+151} \text{ eV}$,	$norm_4 = 209_{-55}^{+47}$,	$F_X = 0.15$
$[C/D] = 16_{-7}^{+23} \times 10^{-5}$, $[O/D] < 1.2 \times 10^{-5}$		
$[Fe/D] = 1.12_{-0.20}^{+0.35} \times 10^{-5}$		
power-law model:		$F_X = 0.016$
$\Gamma^\dagger = 2.35_{-0.10}^{+0.14}$, $norm = 2.73_{-2.18}^{+3.07}$		
gaussian model:		$F_X = 0.005$
$E_1 = 2309_{-16}^{+15} \text{ eV}$,	$\sigma_1 = 105_{-18}^{+21} \text{ eV}$,	$S_1^\ddagger = 0.98_{-0.21}^{+0.20}$
$E_2 = 5444_{-63}^{+71} \text{ eV}$,	$\sigma_2 = 165_{-82}^{+163} \text{ eV}$,	$S_2 = 0.049_{-0.009}^{+0.020}$
$E_3 = 6386_{-42}^{+45} \text{ eV}$,	$\sigma_3 = 124_{-64}^{+76} \text{ eV}$,	$S_3 = 0.053_{-0.014}^{+0.015}$

† Spectral photon index.

‡ photons $\text{cm}^{-2} \text{ s}^{-1}$.

(Errors are 90% confidence level)

the iron ions exist in the plasma as an impurity, and that they are collisionally interacting with thermal electrons. The iron abundance to deuterium ions is evaluated to be $[Fe/D] = 1.1 \times 10^{-5}$, which is comparable to $[C/D]$ or $[O/D]$ measured in the VUV band [5]. It is anticipated that high Z impurities enter the plasma due to the sputtering caused by the plasma-wall interaction.

Actually, Cr-L line data are not included in the MEKAL model, which is partly responsible for the fit residuals around the Fe-L. It also need attention that the MEKAL model assumes the collisional equilibrium, whereas it is marginal for TPE-RX. As shown in Table 1, $[C/D]$ and $[O/D]$ are constrained from the X-ray spectrum, too. However, their abundances are determined in the energy range where our device has very little detective efficiency, hence the systematic error is probably significant. It is essential to replace the X-ray window with C- or O-free material, such as thin beryllium ($\sim 1 \mu\text{m}$).

We thank Prof. Kuni Masai for useful discussions and comments.

References

- [1] K.D. Irwin, PhD thesis, Stanford Univ., (1995).
- [2] K.D. Irwin *et al.*, IEEE. Trans. Appl. Supercond. **5**, 2690 (1995).
- [3] Y. Ishisaki *et al.*, Proc. SPIE **5501**, 123 (2004).
- [4] K. Mitsuda, Proc. SPIE **5488** (2004).
- [5] Y. Ishisaki *et al.*, Proc. SPIE **4851**, 831 (2003).
- [6] D. McCammon *et al.*, Astrophys. J. **576**, 188 (2002).
- [7] Y. Yagi *et al.*, Fusion Eng. Des. **45**, 409 (1999).
- [8] Y. Yagi. Nucl. Fusion **40**, 1933 (2000).
- [9] Y. Takei *et al.*, Nucl. Instrum. Methods Phys. Res. A **523**, 134 (2004).
- [10] A.E. Szymkowiak *et al.*, J. Low Temp. Phys. **93**, 281 (1993).
- [11] R. Mewe *et al.*, Astron. Astrophys. Suppl. Ser. **62**, 197 (1985).
- [12] H. Koguchi *et al.*, Jpn. J. Appl. Phys. Suppl. **43**, 1159 (2004).